Available online at www.sciencedirect.com
ScienceDirect
journal homepage: www.elsevier.com/locate/bbe

Original Research Article

Contralateral asymmetry for breast cancer detection : A CADx approach

Q1 Jose M. Celaya-Padilla [a,*], Cesar H. Guzmán-Valdivia [a], Carlos E. Galván-Tejada [b], Jorge I. Galván-Tejada [b], Hamurabi Gamboa-Rosales [c], Idalia Garza-Veloz [c], Margarita L. Martinez-Fierro [c], Miguel A. Cid-Báez [c], Antonio Martinez-Torteya [d], Francisco J. Martinez-Ruiz [b], Huizilopoztli Luna-García [b], Arturo Moreno-Baez [b], Amita Nandal [e]

[a] CONACyT, Universidad Autónoma de Zacatecas, Jardín Juarez 147, Centro, 98000 Zacatecas, Zacatecas, Mexico
[b] Unidad Académica de Ingeniería Eléctrica, Universidad Autónoma de Zacatecas, Jardín Juarez 147, Centro, 98000 Zacatecas, Zacatecas, Mexico
[c] Unidad Académica de Medicina Humana y Ciencias de la Salud, Universidad Autónoma de Zacatecas, Jardín Juarez 147, Centro, 98000 Zacatecas, Zacatecas, Mexico
[d] Universidad de Monterrey, Avenida Ignacio Morones Prieto 4500 Pte., Jesús M. Garza, 66238 San Pedro Garza García, Nuevo Leon, Mexico
[e] University of Science and Information Technology, Ohrid, Macedonia

ARTICLE INFO

Article history:
Received 30 May 2017
Received in revised form
30 September 2017
Accepted 27 October 2017
Available online xxx

Keywords:
Brest cancer
Contralateral
CADx
Machine learning
Detection
Asymmetry

ABSTRACT

Early detection is fundamental for the effective treatment of breast cancer and the screening mammography is the most common tool used by the medical community to detect early breast cancer development. Screening mammograms include images of both breasts using two standard views, and the contralateral asymmetry per view is a key feature in detecting breast cancer. However, most automated detection algorithms do not take it into account. In this research, we propose a methodology to incorporate said asymmetry information into a computer-aided diagnosis system that can accurately discern between healthy subjects and subjects at risk of having breast cancer. Furthermore, we generate features that measure not only a view-wise asymmetry, but a subject-wise one. Briefly, the methodology co-registers the left and right mammograms, extracts image characteristics, fuses them into subject-wise features, and classifies subjects. In this study, 152 subjects from two independent databases, one with analog- and one with digital mammograms, were used to validate the methodology. Areas under the receiver operating characteristic curve of 0.738 and 0.767, and diagnostic odds ratios of 23.10 and 9.00 were achieved, respectively. In addition, the proposed method has the potential to rank subjects by their probability of having breast

Q2 * *Corresponding author at*: CONACyT, Universidad Autónoma de Zacatecas, Jardín Juarez 147, Centro, 98000 Zacatecas, Mexico.
E-mail address: jose.celaya@uaz.edu.mx (J.M. Celaya-Padilla).

https://doi.org/10.1016/j.bbe.2017.10.005

Please cite this article in press as: Celaya-Padilla JM, et al. Contralateral asymmetry for breast cancer detection: A CADx approach. Biocybern Biomed Eng (2017), https://doi.org/10.1016/j.bbe.2017.10.005

cancer, aiding in the re-scheduling of the radiologists' image queue, an issue of utmost importance in developing countries.

1. Introduction

Breast cancer represents nearly one-third of all female cancer cases in the United States [1] and is one of the global leading causes of death among women [2]. Early detection is fundamental for the effective treatment of breast cancer, and furthermore, it has been proven to help reduce mortality rates by up to 65% [3–5]. Currently, this is done with the aid of some type of medical imaging technique, such as mammography, ultrasound, magnetic resonance imaging (MRI), positron emission tomography (PET), tomosynthesis, and thermography [3].

Lately, thermography has gained some attention, since it is a non-invasive and non-contact imaging technique. Instead of using ionizing radiation, venous access, or other invasive procedure, it uses the infrared electromagnetic radiation emitted by the human body, which is captured by a thermographic camera and analyzed by a computer-aided system. Among the studies that use thermography images to classify between subjects with and without breast cancer, Ng and Fok [6] and Ng et al. [7] reported sensitivities of 0.689 and 0.812, and specificities of 0.400 and 0.882, respectively. The screening tomosynthesis has also gained popularity, mainly due to the fact that it may improve the detection rate and decrease the amount of false positive cases detected [8]. Houssami et al. [9] compared screen-detection measures for single-reading of tomosynthesis against double-reading mammograms, and results showed a cancer detection rate of 8.2 vs. 6.3 per 1000 screens.

Nevertheless, globally, and specially in developed countries, the screening mammography is still the most common tool used by the medical community to detect early breast cancer development. Mammograms allow clinicians to inspect each breast in two standard views, craniocaudal (CC) and mediolateral oblique (MLO), where tissue abnormalities such as calcifications, masses, and architectural distortions associated with the early development of breast cancer can be visualized [3]. Furthermore, in recent years, great efforts have been made to develop computer-aided detection (CADe) and diagnosis (CADx) systems to assist radiologists in interpreting digital mammograms [10–13]. Namely, CADe and CADx systems are being developed in order to aid specialists in the detection of tissue abnormalities. However, detecting such abnormalities represent a challenging task due to the low signal-to-noise ratio of the mammograms, the heterogeneous tissue content of the breasts, as well as their size and shape, and the size, shape, and location of the abnormalities [14–16].

CADe systems have been shown to be very sensitive in detecting breast abnormalities [17,18], but these systems tend to have low specificities, producing a large number of false positives that yield an increased amount of unnecessary biopsies. Moreover, current methodologies detect masses and/or calcifications not accurately aligned with the abnormalities, misleading the radiologists [15,19,20]. Nevertheless, several researchers are currently working to enhance the performance of CADe systems. An example of this can be found in the work done by de Sampaio et al. [21], in which they aimed at detecting masses. First, they classified breasts as either dense or non-dense using an adaptive algorithm. Then, they used a micro-genetic algorithm to create a texture proximity mask with which suspicious regions were localized. Lastly, they reduced the amount of false positive regions using two different approaches, one with a density-based spatial clustering and a proximity ranking of the textures extracted from the suspicious regions, and the other with a texture analysis by the combination of phylogenetic trees, local binary patterns, and support vector machines (SVM). They produced sensitivities of 0.837 and 0.930, and a rate of 0.19 and 0.15 false positives per image, for the dense and non-dense breasts, respectively. Dhungel et al. [16] also presented a CADe/CADx system for the detection of masses. Using a cascade of deep learning methods refined using Bayesian optimization, this system detected 90% of masses at a rate of 1 false positive per image.

On the other hand, CADx systems can be used by radiologists as a second opinion [2,22,23] and may help in reaching a correct interpretation of abnormal findings, thus, reducing the amount of unnecessary biopsies [10,14,19,22,24]. In this regard, the previously discussed work by Dhungel et al. [16] was able to classify masses as either malignant or benign with a sensitivity of 0.90 and a specificity of 0.7. Similarly, Raghavendra et al. [25] presented an automated classification system based on Gabor wavelets, locality sensitive discriminant analysis, and a k-nearest neighbor classifier. This system yielded a mean accuracy, sensitivity, and specificity of 0.987, 0.993, and 0.983, respectively.

But, the detection of breast abnormalities can be enhanced by comparing different images of the same subject, either from the same breast at different time points [26] or by contralateral asymmetry analyses that measure the differences between the left and right breasts at a specific time point [27,28]. Furthermore, it has been shown that the contralateral asymmetry may be a risk factor for breast cancer. Nevertheless, due to the challenges that measuring such an asymmetry implies, most of the automated detection approaches to date do not take contralateral asymmetry into account [29].

Current asymmetry detection methods are often based on simple bilateral subtraction techniques [26,30]. However, breasts are composed of highly heterogeneous and deformable tissue, resulting in an unlikely perfect match between both breasts [27]. To avoid this problem, Miller and Astley [31] proposed a technique for the detection of asymmetry using a semi-automated texture-based procedure for the segmentation of the glandular tissue, measuring the shape between

Please cite this article in press as: Celaya-Padilla JM, et al. Contralateral asymmetry for breast cancer detection: A CADx approach. Biocybern Biomed Eng (2017), https://doi.org/10.1016/j.bbe.2017.10.005

views for detection of the occurrence of asymmetry, obtaining an accuracy of 0.867 on a validation data set of 30 screening mammogram pairs. Later, Miller and Astley [32] presented a system based on measures of shape, topology, and distribution of brightness. The method was tested on 104 mammogram pairs, and a classification accuracy of 0.74 was obtained. Similarly, Ferrari et al. [33] developed a method using directional filtering with Gabor wavelets at different orientations and scales. There, asymmetry was characterized by variations in oriented textural patterns. Validated in a data set of 80 subjects, they achieved a classification accuracy rate of 0.744%. More recently, Torrents-Barrena et al. [34] also used a Gabor-based detection coupled to an SVM classification stage, yielding an area under the receiver operating characteristic (ROC) curve (AUC) ranging from 0.724 to 0.827. Recently Evans et al. [35] demonstrated that cancer signal information is present in the contralateral breast where the tumor was originally diagnosed, but despite this, CADe/CADx systems do not fully incorporate the contralateral/asymmetry information into their process.

The objective of this work was to develop a CADx methodology that incorporates information from both breasts, as well as their contralateral asymmetry, in order to automatically classify subjects as either healthy or in risk of having breast cancer. Additionally, we aimed at ranking subjects within a subset by their risk of having breast cancer, a characteristic that would make this CADx system of great importance in developing countries, where radiologists have workloads that exceed their capabilities. This methodology, based on previous efforts [36], co-registers the left and right images, extracts image features, and performs a classification enhanced by a robust feature selection algorithm. Moreover, we propose the use of subject-wise features in order to avoid side- and view-dependency and to create subject-specific prediction models, instead of region-specific predictions. This methodology was validated in two independent publicly available data sets containing both digital and analog mammograms.

This paper is organized as follows: Section 2 presents the proposed methodology in detail, Section 3 reports the results of the experiments, which are thoroughly discussed in Section 4, and final conclusions are presented in Section 5.

2. Materials and methods

An overview of the proposed methodology is shown in Fig. 1. Briefly, the mammograms of each subject were first pre-processed and segmented in order to analyze the breast tissue alone. Then, the left mammograms (CC and MLO) were registered into their corresponding right mammograms using a B-Spline algorithm, which aligned both images in the same coordinate plane. A pixel-wise subtraction was then carried on between the co-registered images, yielding a CC and an MLO contralateral asymmetry image per subject. Four enhancement filters were then applied to the asymmetry images, and several features were extracted from each. These view-specific features were combined in order to obtain subject-specific features. Finally, using robust machine learning algorithms, a diagnostic model able to classify subjects was generated.

2.1. *Image processing*

2.1.1. *Segmentation*

The automatic segmentation of the breast tissue was based on the estimation of the background noise. An initial segmentation mask was created by estimating the background noise in the image and discarding all pixels below five standard

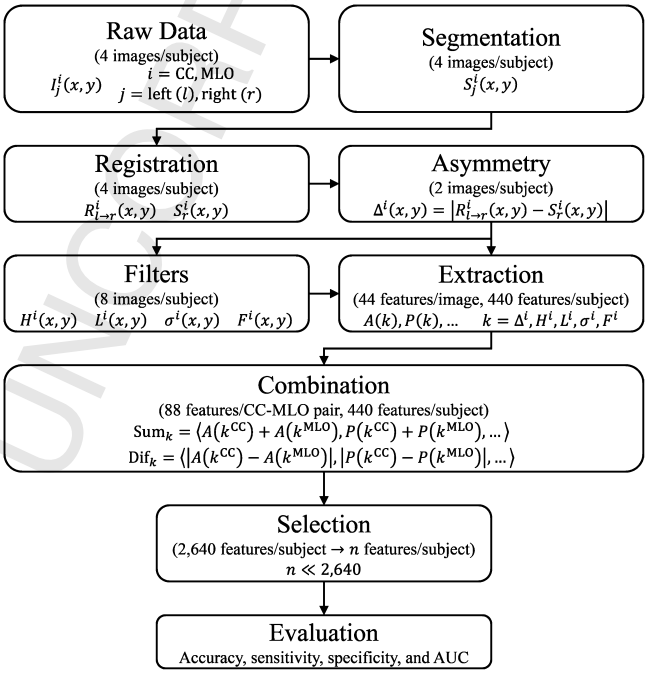

Fig. 1 – Overview of the proposed methodology.

Please cite this article in press as: Celaya-Padilla JM, et al. Contralateral asymmetry for breast cancer detection: A CADx approach. Biocybern Biomed Eng (2017), https://doi.org/10.1016/j.bbe.2017.10.005

deviations of the noise level. Then, holes were removed by applying erosion and dilation morphological operations with a 3×3 supporting region, as defined in:

$$S_j^i(x,y) = (I_j^i(x,y) \oplus B(x,y)) \ominus B(x,y), \quad (1)$$

where $S_j^i(x,y)$ and $I_j^i(x,y)$ represent the segmented and raw images for the ith view, either CC or MLO, and the jth side, either left (l) or right (r), respectively; $\oplus$ and $\ominus$ are the dilation and erosion morphological operations, respectively; and $B(x,y)$ is a 3×3 structural element. The largest region was used as the segmentation mask while all other high intensity regions were removed from the images.

2.1.2. *Registration*

As previously mentioned, the breast is a highly heterogeneous organ whose appearance can physiologically change significantly between sessions. Additional dissimilarities between images, related to patient movement, sensor noise, different radiation exposure, or variation of breast compression also makes this comparison difficult. Therefore, in order to efficiently compare two mammograms, an initial alignment using an image registration algorithm had to be carried out. We performed a free-form deformation (FFD) based on B-splines. B-Spline deformable registration is based on deforming an image by modifying a mesh of control points following a maximization of a similarity measure [37,26]. For 2D images, such as the mammograms involved in this study, B-splines can be modeled by the tensor product of the 1D cubic B-splines. A 2D non-rigid transformation can be written as: $T(r_p) = r_p + d(r_p)$, where r_p represents the x and y coordinates of the pth pixel and $d(r_i)$ the deformation it suffers. The 2D deformation was modeled as $d(r_p) = \langle d^x(r_p), d^y(r_p) \rangle$ using the tensor product of β, the nth-order B-splines, as follows:

$$d^q(r_p) = \sum_{i,j} c_{i,j}^q \beta\left(\frac{x}{m_x} - i\right) \beta\left(\frac{y}{m_y} - i\right) \quad (2)$$

where $d^q(r_p)$ represents the deformation of the pth pixel in the qth axis plane (x or y), $c = c_{ij}^q$ is the deformation coefficient for the qth plane, and m_q is the knot spacing in the qth direction. The deformation coefficients were estimated by maximizing the similarity metric ψ, according to:

$$c_{i,j}^q = \underset{q}{\arg\max}\, \psi\langle S_r^i(x,y), S_l^i(x,y) \rangle \quad (3)$$

For this study, a multi-resolution B-Spline pyramid approach was used [36,38]. First, the left segmented mammograms were horizontally flipped. Then, both the flipped left images (CC and MLO) and their right non-flipped counterparts were re-sampled into lower resolution images. Next, the pyramids for the multi-resolution were generated and registration was performed. The left segmented mammograms were deformed using the final parameters of the registration, where a mutual information metric [39] was used as the similarity metric ψ.

2.1.3. *Contralateral asymmetry*

Once the images were co-registered, and in order to enhance the differences between the breasts, a pixel-wise absolute difference was computed between each left-right pair of mammograms, resulting in asymmetry images $\Delta^i(x,y)$, defined as:

$$\Delta^i(x,y) = \left| R_{l \to r}^i(x,y) - S_r^i(x,y) \right| \quad (4)$$

where $R_{l \to r}^i(x,y)$ represents the left to right registered image for the ith view. Fig. 2 shows an example of a mammogram that was co-registered and subtracted in order to highlight the bilateral differences.

2.1.4. *Enhancement filters*

To study the appearance of the architectural distortions, two enhancing filters were applied to the asymmetry images, a morphological high frequency enhancement filter $M^i(x,y)$ designed to enhance fiber-like tissues, and a Laplacian of Gaussian filter $L^i(x,y)$ that enhanced high frequency patterns. Additionally, since the texture between normal and abnormal tissues is different [40], two texture maps were created. The map $\sigma^i(x,y)$ computed the local standard deviation of the

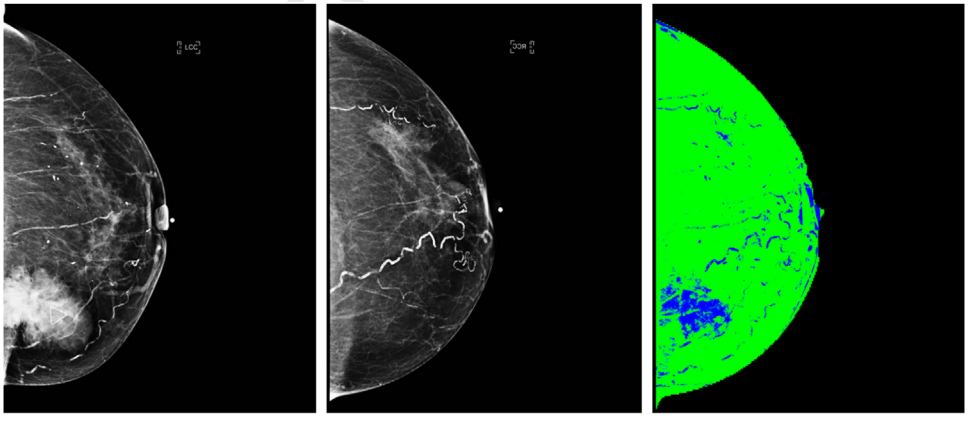

(a) (b) (c)

Fig. 2 – Bilateral differences. (a) Shows a segmented mammography of a right breast, (b) its left to right registered counterpart, and (c) a color map of the resulting asymmetry image, where left and blue indicate small and large bilateral differences, respectively.

Please cite this article in press as: Celaya-Padilla JM, et al. Contralateral asymmetry for breast cancer detection: A CADx approach. Biocybern Biomed Eng (2017), https://doi.org/10.1016/j.bbe.2017.10.005

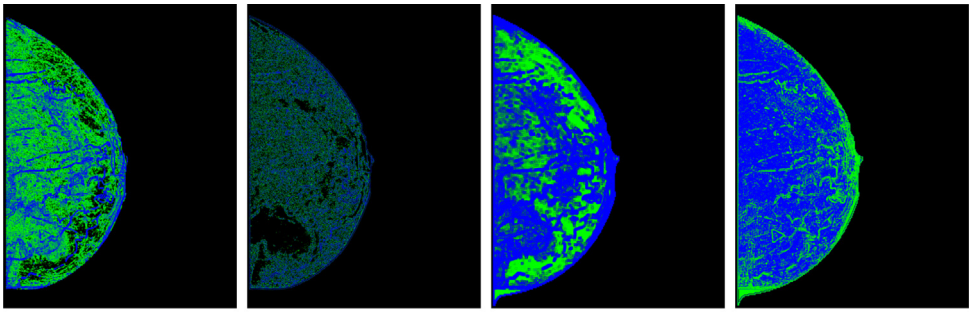

Fig. 3 – Enhancement filters. Color map of the (a) morphological high frequency $M^i(x, y)$, (b) Laplacian of Gaussian $L^i(x, y)$, (c) local standard deviation $\sigma^i(x, y)$, and (d) local fractal dimension $F^i(x, y)$ filters. Green and blue pixels represent low and high intensity values, respectively.

mammography images, and the map $F^i(x, y)$ the local fractal dimension. Image processing was implemented in C++ using ITK libraries for image manipulation [41] following the previous implementation presented in [36]. Image 3 shows an example of each one of these filters.

2.1.5. *Feature extraction*

A main step in any kind of pattern recognition problem is the representation of data, in this case the characterization of the breast tissue and their properties [42]. There are several features that may be quantified aiming to detect early signs of cancer, following our previous efforts [36], we propose the study of 44 features that are related to either the morphology of the breasts or to the information found in the signal of the images. All features are described in Table 1.

2.1.6. *Feature combination*

In order to go from view-specific features into subject-specific features we propose the combination of each pair of CC and MLO features by adding and subtracting them, as defined by:

$$\begin{aligned} f_n^+(k) &= f_n(k^{CC}) + f_n(k^{MLO}) \\ f_n^-(k) &= \left| f_n(k^{CC}) - f_n(k^{MLO}) \right| \end{aligned} \tag{5}$$

As described in Fig. 1, 88 subject-specific features were extracted per pair of CC and MLO images, resulting in a total of 440 features per subject.

2.1.7. *Feature selection*

In recent years, several feature selection methodologies have been studied for breast cancer detection. Algorithms such as LASSO, KNN, SVM and others have been widely used due to their performance [43,44], but as of today, there is not a *golden method* that outperforms any other classifier in every task. We previously compared the performance of several classifiers [43,44,36]. Following our findings, we propose the use of FRESA.CAD. FRESA.CAD is an R package that uses a bootstrapped stage-wise model selection (B:SWiMS) algorithm. FRESA.CAD internally computes LASSO, KNN, B:SWIMS, B:SWIMS with bagging, and B:SWIMS ensembled. Therefore, we were able to compare in a single procedure the efficiency of the methodology in a wide range of feature selection algorithms at the same time, with exactly the same conditions in the train and validation stages. Further details of the FRESA.CAD package can be found in http://cran.r-project.org/web/packages/FRESA.CAD/index.html.

2.2. *Data acquisition*

In this research, two publicly available data sets were used: The Digital Database for Screening Mammography (DDSM) and the Breast Cancer Digital Repository (BCDR). DDSM [45] is one of the largest public mammogram databases, it has been used in over 500 research projects (up to 2016). This database has 2620 cases distributed as follows: 625 healthy subjects, 1011 benign cases, and 914 malign cases. It includes two standardized CC and MLO mammograms per subjects, and was constructed by taking film-based mammograms that were then digitized using four different scanners: DBA, HOWTEK-A, LUMISYS, and HOWTEK-D. BCDR is a fairly newer public database [46]. It is maintained by the IMED Project (Development of Algorithms for Medical Image Analysis), which was created and updated by the INEGI, FMUP-CHSJ, and CETA-CIEMAT, from 2009 to 2013. The BCDR is a 100% digital mammogram database, it has 774 subjects (723 women and 1 male), from an age range between 27 years and 92 years. The images are stored in a TIFF format at 14 bits, and the type of scanner is undisclosed.

From the above mentioned data sets, we used the Lumisys subset from the DDSM data set and the whole BCDR data set. Using this data sets we created two categories, healthy subjects and non-healthy subjects. The latter refer to those with proven cancer (i.e. masses, calcification, distortions, etc.) and benign abnormalities of any type. The data sets were adjusted to exhibit the same ratio between the healthy and non-healthy groups, yielding a total of 152 subjects. Table 2 shows the detail of the data used in this research.

2.3. *Experiment design*

Two experiments were performed, one for each data set. Features were first z-normalized using a rank-based inverse normal transformation [47]. Afterwards, correlation between pairs of features was evaluated, and for each pair of highly

Please cite this article in press as: Celaya-Padilla JM, et al. Contralateral asymmetry for breast cancer detection: A CADx approach. Biocybern Biomed Eng (2017), https://doi.org/10.1016/j.bbe.2017.10.005

Table 1 – Features extracted from each asymmetry image.

Category	Feature	Definition
Shape	Surface area	$A_R(k) = \sum_{(x,y)\in k} a_{x,y}$
	Perimeter	$P(k) = \sum_{i\in\epsilon(k)} d(e_i, e_{i+1})$
	Compactness	$C(k) = \frac{P(k)^2}{A(k)}$
	Elongation	$E(k) = \frac{\text{argmax}_q L_q}{\text{argmin}_q L_q}$
	[2]Region centroid	$q\tilde{A}_R(k) = \langle x\tilde{A}_R(k) = \frac{m_{10}}{m_{00}}, y\tilde{A}_R(k) = \frac{m_{01}}{m_{00}}\rangle$
	[3]Region scatter	$S_R(k) = \langle \frac{m_{20}}{m_{00}} - x\tilde{A}_R^2, \frac{m_{11}}{m_{00}} - x\tilde{A}_R y\tilde{A}_R, \frac{m_{20}}{m_{02}} - y\tilde{A}_R^2\rangle$
Signal	Mean	$\mu(k) = \sum_{i=0}^{\text{maxi}} i p_i(k)$
	Median	$v_{50}(k)$
	Energy	$E(k) = \sum_{i=0}^{\text{maxi}} i^2 p_i(k)$
	Variance	$\sigma^2(k) = E^2(k) - \mu^2(k)$
	Standard deviation	$\sigma(k) = \sqrt{\sigma^2(k)}$
	Dynamic range	$DR(k) = \text{argmax}_{\forall(x,y)\in k}\, i_{x,y} - \text{argmin}_{\forall(x,y)\in k}\, i_{x,y}$
	z-mean	$\overline{z}(k) = \frac{\mu(k)}{\sigma(k)}$
	Entropy	$H(k) = \sum_{i=0}^{\text{maxi}} p_i(k)\log p_i(k)$
	Skewness	$\gamma(k) = \sum_{i=0}^{\text{maxi}} p_i(k)\left(\frac{i-\mu(k)}{\sigma(k)}\right)^3$
	Kurtosis	$\beta(k) = \sum_{i=0}^{\text{maxi}} p_i(k)\left(\frac{i-\mu(k)}{\sigma(k)}\right)^4 - 3$
	z-Range	$z_{DR}(k) = \frac{DR(k)}{\sigma(k)}$
	[2]Fraction $<\sigma$	$p_{i<\sigma}(k) = \langle \sum_{i=0}^{v_{2\sigma}(k)} p_i(k), \sum_{i=0}^{v_{3\sigma}(k)} p_i(k)\rangle$
	[2]Fraction $>\sigma$	$p_{i<\sigma}(k) = \langle \sum_{i=v_{2\sigma}(k)}^{\text{maxi}} p_i(k), \sum_{i=v_{3\sigma}(k)}^{\text{maxi}} p_i(k)\rangle$
	[10]Percentile	$v_n(k) : n = \langle 0.01, 0.1, a, e, 10, 25, 75, 90, 95, 99, 99.9, 99.99\rangle$
	Trimmed mean	$\mu_t(k) = \sum_{i=v_5(k)}^{v_{95}(k)} i p_i(k)$
	Trimmed σ	$\sigma_t(k) = \left[\sum_{i=v_5(k)}^{v_{95}(k)} (i-\mu_t(k))^2 p_i(k)\right]^{1/2}$
	Trimmed z-mean	$\overline{z}_t(k) = \frac{\mu_t(k)}{\sigma_t(k)}$
	Total signal	$M_{0,0} = \sum_{\forall(x,y)\in k} i_{x,y}$
	[2]Signal centroid	$q\tilde{A}_S(k) = \langle x\tilde{A}_S(k) = \frac{M_{10}}{M_{00}}, y\tilde{A}_S(k) = \frac{M_{01}}{M_{00}}\rangle$
	[2]Signal scatter	$S_s(k) = \langle \frac{M_{20}}{M_{00}} - x\tilde{A}_S^2, \frac{M_{11}}{M_{00}} - x\tilde{A}_S y\tilde{A}_S, \frac{M_{20}}{M_{02}} - y\tilde{A}_S^2\rangle$
	Signal surface	$A_S = \Delta_{xy}\left(\Delta_{xy}^2 + 4\left(i_{x,y} - q\tilde{A}_S(k)\right)^2\right)^{1/2}$

Numbers in superscript indicate the times a feature was measured, those without a superscript were measured once; $a_{x,y}$ is the unit area of a pixel; $d(e_i, e_{i+1})$ is the Euclidean distance between the ith and the ith + 1 neighboring edge points found in the set of edge points $\epsilon(k)$; L_q is the length of the bounding boxing the q axis; $m_{i,j}$ $M_{i,j}$ and the moment functions of the shape and the signal of k, respectively; $i_{x,y}$ is the intensity of the pixel at the x, y coordinates and $p_i(k)$ is the relative frequency of the ith intensity; $v_n(k)$ is the intensity of the pixel located at the nth% position of the ordered intensities of k; and $\Delta_{x,y}$ is the image size.

correlated features (Pearson correlation larger than 0.9), one of such features was removed. Then, the feature selection procedure was performed using a 10-fold cross-validation repeated 20 times. This was done to avoid bias towards a specific data set partition. False discovery rate was set to 0.025 to avoid non-statistical significant features to be incorporated into the models.

3. Results

In order to have a full spectrum of the performance for the proposed methodology, accuracy, area under the receiver operator characteristic (ROC) curve (AUC), sensitivity, and diagnostic odds ratio (dOR) were computed at different specificities (best, 0.5, 0.8, 0.9). Tables 3 and 4 show the results for the proposed methodology, and Figs. 4 and 5 show the ROC curve for the proposed methodology, for the BCDR and the DDSM data sets, respectively. All the results shown were computed using the ensembled prediction of the test, the one taking into account the results from the 20 iterations of the feature selection procedure.

The model selection strategy yielded reproducible models of healthy vs. non-healthy subjects with an AUC of 0.738 for the BCDR data set. An ODDS ratio of 23.10 was achieved along

Please cite this article in press as: Celaya-Padilla JM, et al. Contralateral asymmetry for breast cancer detection: A CADx approach. Biocybern Biomed Eng (2017), https://doi.org/10.1016/j.bbe.2017.10.005

Table 2 – Distribution of mammograms.

Subset	Healthy	Non-healthy	Total
DDSM-Lumisys	32	56	88
BCDR	23	41	64
Total	55	97	152

Table 3 – Healthy vs. non-healthy. Final model performance in the BCDR data set.

Model	Accuracy	AUC	Sensitivity	Specificity	dOR
BSWIMS					
Best	0.672	0.738	0.512	0.957	23.100
specificity@0.5	0.586	0.738	0.634	0.500	1.733
specificity@0.8	0.647	0.738	0.561	0.800	5.111
specificity@0.9	0.667	0.738	0.537	0.900	10.421
KNN					
Best	0.563	0.683	0.366	0.913	6.058
specificity@0.5	0.662	0.683	0.753	0.500	3.049
specificity@0.8	0.569	0.683	0.440	0.800	3.141
specificity@0.9	0.563	0.683	0.374	0.900	5.386
LASSO					
Best	0.688	0.655	0.707	0.652	4.531
specificity@0.5	0.633	0.655	0.707	0.500	2.417
specificity@0.8	0.538	0.655	0.390	0.800	2.560
specificity@0.9	0.511	0.655	0.293	0.900	3.724

Table 4 – Healthy vs. non-healthy. Final model performance in the DDSM data set.

Model	Accuracy	AUC	Sensitivity	Specificity	dOR
BSWIMS					
Best	0.750	0.767	0.750	0.750	9.000
specificity@0.5	0.682	0.767	0.786	0.500	3.667
specificity@0.8	0.689	0.767	0.625	0.800	6.667
specificity@0.9	0.634	0.767	0.482	0.900	8.379
KNN					
Best	0.693	0.758	0.589	0.875	10.043
specificity@0.5	0.698	0.758	0.811	0.500	4.297
specificity@0.8	0.686	0.758	0.621	0.800	6.541
specificity@0.9	0.580	0.758	0.396	0.900	5.911
LASSO					
Best	0.773	0.838	0.696	0.906	22.176
specificity@0.5	0.750	0.838	0.893	0.500	8.333
specificity@0.8	0.734	0.838	0.696	0.800	9.176
specificity@0.9	0.770	0.838	0.696	0.900	20.647

with a sensitivity of 0.512 and a specificity of 0.957. The bilateral model achieved a high specificity, making the Bilateral model highly suitable to detect the abnormalities. Classic KNN and LASSO feature selection methodologies achieved similar AUC results, nevertheless with a ODDS ratio of only 6.058 and 4.531 respectively.

The ROC curve analysis for the BCDR data set is shown in Fig. 4, as we can see the ensemble prediction of the three feature selection algorithms have a similar performance with AUC ranging from 0.738, 0.683, 0.655 for B:SWiMS, KNN, and LASSO respectively. As we can see the use of *patient features* yields to reproducible models that can be used to triage the detection of abnormalities related to breast cancer.

On the other hand, the model selection B:SWiMS strategy when used on the healthy vs. Other abnormalities in the DDSM data set achieved an ensemble test AUC of 0.767. An ODDS ratio of 9.00 was achieved along with a sensitivity of 0.750 and a specificity of 0.750. as in the previous data set, the KNN and LASSO feature selection methodologies achieved similar AUC results, here, the ODDS ratio increased to a 10.043 and 22.176 respectively. The ROC curve analysis for the DDSM data set is shown in Fig. 4, the ensemble prediction of the three feature selection algorithms have a similar performance with AUC ranging from 0.767, 0.758 and 0.838 for B:SWiMS, KNN, and LASSO respectively. As we can see the use of *patient features* yields to reproducible models that can be used to triage the detection of abnormalities related to breast cancer.

Please cite this article in press as: Celaya-Padilla JM, et al. Contralateral asymmetry for breast cancer detection: A CADx approach. Biocybern Biomed Eng (2017), https://doi.org/10.1016/j.bbe.2017.10.005

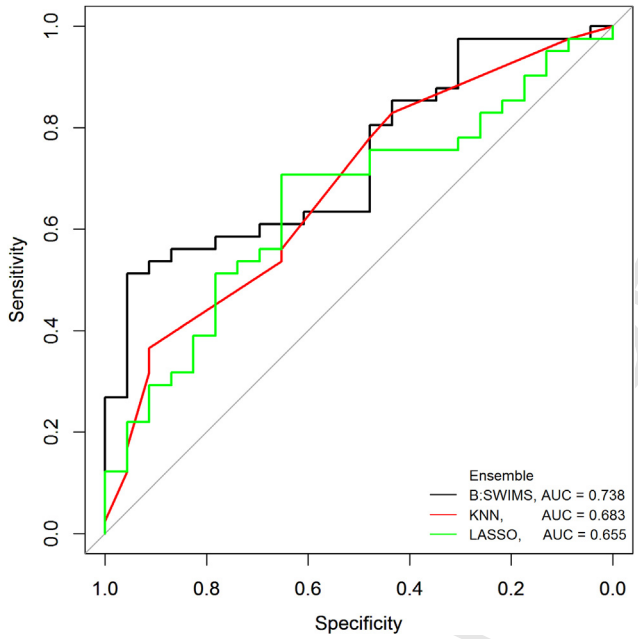

Fig. 4 – ROC curves for the healthy vs. non-healthy classification in the BCDR data set.

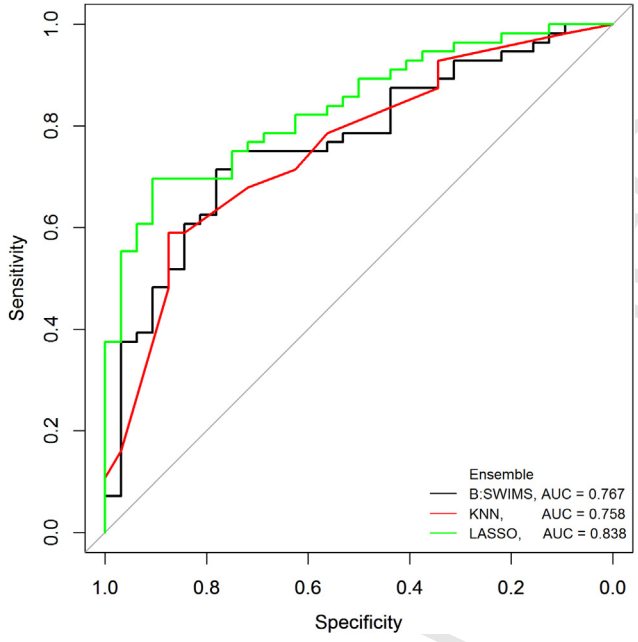

Fig. 5 – ROC curves for the healthy vs. non-healthy classification in the DDSM data set.

4. Discussion

Despite working with two different sets of images, one digital and one analog, the proposed registration methodology was able to successfully align the contralateral images. Once the images were aligned, the bilateral image subtraction generated an asymmetry image, which was enhanced with four different filters. Then, 880 subject-specific features were extracted. The creation of new features by merging the CC and MLO views helped to eliminate the dependency on view. The model selection strategy yielded reproducible models of healthy vs. non-healthy subjects for the BCDR and DDSM data sets. The bilateral approach model achieved a high specificity, making the Bilateral model highly suitable to detect any abnormalities and may be used to triage the detection of abnormalities related to breast cancer.

One key feature over previous approaches [33,48,49] is that they only try to detect breast cancer, i.e. only malignant cancer lesion, while our approach combine the benign and malign abnormalities into one category, that imply, the detection of the abnormality from the healthy ones regarding the type of abnormality i.e. (calcification, masses, architectural distortion, etc.) effectively making it a more complex problem, yet, obtaining great results. One of the main reason to combine said lesions, is that if leaved untreated benign abnormalities, they may evolve into malign lesions. The proposed methodology is fully automated, there is no need for human intervention as other approaches [50]. The proposed CADx system targets develop countries where the access to medical care is limited, and there is a deficit of trained radiologists, therefore a tool that successfully ranks the subjects according to the changes of having breast cancer related abnormalities may reduce the mortality rate. Moreover the models created using the patient features use subjects features rather than side specific mammograms as in other approaches. Even with different feature selection algorithms, LASSO, KNN, and B:SWIMS the performance was similar. This similar performance suggests that the proposed methodology is not specific to a particular feature selection algorithm. Moreover the achieve ODDS ratio of the presented model suggest a high association.

Please cite this article in press as: Celaya-Padilla JM, et al. Contralateral asymmetry for breast cancer detection: A CADx approach. Biocybern Biomed Eng (2017), https://doi.org/10.1016/j.bbe.2017.10.005

Table 5 – Similar approaches comparison.

Author	Asymmetry approach	Type	Performance
Rodriguez-Rojas et al. [51]	Bilateral asymmetry used to classify low/high risk mammograms (bi-rads based) – genetic algorithm as feature selection	Feature-based	AUC = 0.88
Martí et al. [49]	Use only MLO mammograms to classify abnormal/normal cases, bilateral feature-based, random forest-LOOCV	Temporal registration based	AUC = 0.76
Zheng et al. [26]	Bilateral density asymmetry to classify high risk patients, temporal study	No registration	AUC = 0.761
Wang et al. [28]	Feature-based bilateral asymmetry to classify low/high risk mammograms, ANN, no registration	Feature-based	AUC = 0.75
Tan et al. [52]	Near-term breast cancer prediction, using feature based asymmetry SVM	Feature-based	AUC = 0.72
Yin et al. [50]	Detection of masses, bilateral subtraction	Manual registration	A 95 % TP with a 3FP × image
Our approach	Detection of any type of abnormalities (MC, masses, etc.), bilateral subtraction	Automated registration	Two independent datasets with AUC of 0.738 and 0.767 respectively.

In Table 5 a comparison against similar approaches is presented, the authors acknowledge that there are several approaches in the field of breast cancer detection, nevertheless, only approaches that incorporate some type of bilateral analysis were included. In Table 5 we can see, that most of the approaches does not incorporate any sort of alignment prior the comparison, only Yin et al. [50] incorporate manual bilateral registration, while Martí et al. [49] indeed includes automatic registration but is limited to only temporal registration. All other approaches [51,26,27,52] are feature-based only. The presented performance is similar to those that incorporate any asymmetry analysis, nevertheless, our approach was validated in two independent and different type of mammograms (digital and film), even further, those datasets included different ethnicities, while the others were tested only on a single dataset. When comparing our approach with others, we can notice that all others only try to detect breast cancer (i.e. only malignant cancer lesions), while our approach combine the benign and malign abnormalities into one category, that implies, the detection of the abnormality from the healthy ones regarding the type of abnormality, i.e. (calcification, masses, architectural distortion, etc.). Even further, our approach fusions the features from the CC and MLO views, successfully creating a score for each patients while others only output a score for a single mammogram, this approach may output false negatives in some cases where the same breast (i.e. left) may score positive for CC and it may also score negative for the same MLO view, while in our fusion approach the features are patient-based and not bias towards a specific view as others.

This research was performed using a Quad core (8 threads) Xeon processor at 3.0 GHz, 16 GB of RAM, the average time for the image processing stage was 9-11 minutes by each subject, on the feature selection, FRESA.CAD use the FPR to reduce the number of features in each selection stage, the algorithm have a complexity of $O(ndk)$, where n is the cardinality of the training set, d is the dimension of each sample and k is the model size. the average computational time was on average 20 minutes, nevertheless, FRESA.CAD can work on multiple cores at the same time reducing the time according the resources available. The FRESA.CAD time may be somehow long, but the training phase needs to be carryout once.

The proposed methodology exhibits some limitations, among them, there is the necessity of the CC and MLO from the left and right mammograms, this may leave out subjects that undergo only to a specific side mammogram, or women that went under surgical mastectomy and therefore the bilateral analysis can not be performed. Other limitation reside in subjects with breast implants, that due the high radioluminiscent of the implant, it may lead to unrealistic bilateral registration of the breasts, therefore, limiting the use to women without breast implants.

5. Conclusions

The presented CADx methodology yielded to the creation of *patient features* that fusion the information of contralateral asymmetry and the different views into single features. The methodology was validated in two independent data sets using both analog and digital mammograms, and different type of scanners. The achieved results shown that the methodology could classify healthy subjects from any other type of cancer or benign abnormality, to our knowledge it is the first approach that works with any other type of abnormality. The proposed methodology yielded reproducible and similar results even with different model selection strategies. The models have the potential to be used to queue cases with a high chance of malignant findings, effectively reducing the radiologist workload. Such models have the practical use of triaging mammograms in developing countries where there is a deficiency of expert readers.

Future work will focus on validating the methodology on clinical scenarios and the implications of translating this methodology to health systems.

Conflict of interest

The authors declare that there is no conflict of interest regarding the publication of this manuscript.

Please cite this article in press as: Celaya-Padilla JM, et al. Contralateral asymmetry for breast cancer detection: A CADx approach. Biocybern Biomed Eng (2017), https://doi.org/10.1016/j.bbe.2017.10.005

Acknowledgement

J.M.C.P. and C.G.V want to thank the CONACyT, for the support under grant ''CONACyT Cátedra 129 – Convocatoria 2016''.

REFERENCES

[1] DeSantis C, Ma J, Bryan L, Jemal A. Breast cancer statistics, 2013. CA: Cancer J Clin 2014;64:52–62.
[2] Miller AB, Wall C, Baines CJ, Sun P, To T, Narod SA. Twenty five year follow-up for breast cancer incidence and mortality of the Canadian National Breast Screening Study: randomised screening trial. BMJ 2014;348.
[3] Løberg M, Lousdal ML, Bretthauer M, Kalager M. Benefits and harms of mammography screening. Breast Cancer Res 2015;17:63.
[4] Rangayyan RM, Ayres FJ, Leo Desautels JE. A review of computer-aided diagnosis of breast cancer: toward the detection of subtle signs. J Franklin Inst 2007;344:312–48.
[5] Bleyer A, Welch HG. Effect of three decades of screening mammography on breast-cancer incidence. N Engl J Med 2012;367:1998–2005.
[6] Ng EY-K, Fok S-C. A framework for early discovery of breast tumor using thermography with artificial neural network. Breast J 2003;9:341–3.
[7] Ng E, Kee E, Acharya UR. Advanced technique in breast thermography analysis. 27th Annual International Conference of the Engineering in Medicine and Biology Society, IEEE-EMBS 2005. IEEE; 2005. p. 710–3.
[8] Skaane P, Bandos AI, Gullien R, Eben EB, Ekseth U, Haakenaasen U, et al. Prospective trial comparing full-field digital mammography (ffdm) versus combined ffdm and tomosynthesis in a population-based screening programme using independent double reading with arbitration. Eur Radiol 2013;23:2061–71.
[9] Houssami N, Bernardi D, Pellegrini M, Valentini M, Fantò C, Ostillio L, et al. Breast cancer detection using single-reading of breast tomosynthesis (3d-mammography) compared to double-reading of 2d-mammography: evidence from a population-based trial. Cancer Epidemiol 2017;47:94–9.
[10] Doi K. Computer-aided diagnosis in medical imaging: historical review, current status and future potential. Comput Med Imaging Graph 2007;31:198–211.
[11] Lee H, Chen Y-PP. Image based computer aided diagnosis system for cancer detection. Expert Syst Appl 2015;42: 5356–65.
[12] Lo C-M, Chang R, Huang C, Moon W. Computer-aided diagnosis of breast tumors using textures from intensity transformed sonographic images. 1st Global Conference on Biomedical Engineering & 9th Asian-Pacific Conference on Medical and Biological Engineering. Springer; 2015. p. 124–7.
[13] Ganesan K, Acharya UR, Chua CK, Min LC, Abraham KT, Ng K-H. Computer-aided breast cancer detection using mammograms: a review. IEEE Rev Biomed Eng 2013;6:77–98.
[14] Tang J, Rangayyan RM, Xu J, El Naqa I, Yang Y. Computer-aided detection and diagnosis of breast cancer with mammography: recent advances. IEEE Trans Inform Technol Biomedon 2009;13:236–51.
[15] Oliver A, Freixenet J, Marti J, Pérez E, Pont J, Denton ERE, et al. A review of automatic mass detection and segmentation in mammographic images. Med Image Anal 2010;14:87–110.
[16] Dhungel N, Carneiro G, Bradley AP. A deep learning approach for the analysis of masses in mammograms with minimal user intervention. Med Image Anal 2017;37:114–28.
[17] Baker JA, Rosen EL, Lo JY, Gimenez EI, Walsh R, Soo MS. Computer-aided detection (CAD) in screening mammography: sensitivity of commercial CAD systems for detecting architectural distortion. Am J Roentgenol 2003;181:1083–8.
[18] Eadie LH, Taylor P, Gibson AP. A systematic review of computer-assisted diagnosis in diagnostic cancer imaging. Eur J Radiol 2012;81:e70–6.
[19] Dromain C, Boyer B, Ferre R, Canale S, Delaloge S, Balleyguier C. Computed-aided diagnosis (CAD) in the detection of breast cancer. Eur J Radiol 2013;82:417–23.
[20] Kozegar E, Soryani M, Minaei B, Domingues I. Assessment of a novel mass detection algorithm in mammograms. J Cancer Res Therap 2013;9:592.
[21] de Sampaio WB, Silva AC, de Paiva AC, Gattass M. Detection of masses in mammograms with adaption to breast density using genetic algorithm, phylogenetic trees, lbp and svm. Expert Syst Appl 2015;42:8911–28.
[22] Doi K. Current status and future potential of computer-aided diagnosis in medical imaging. Br J Radiol 2014.
[23] Miranda GHB, Felipe JC. Computer-aided diagnosis system based on fuzzy logic for breast cancer categorization. Comput Biol Med 2015;64:334–46.
[24] Dheeba J, Singh NA. Computer aided intelligent breast cancer detection: second opinion for radiologists – a prospective study. Computational Intelligence Applications in Modeling and Control. Springer; 2015. p. 397–430.
[25] Raghavendra U, Acharya UR, Fujita H, Gudigar A, Tan JH, Chokkadi S. Application of gabor wavelet and locality sensitive discriminant analysis for automated identification of breast cancer using digitized mammogram images. Appl Soft Comput 2016;46:151–61.
[26] Zheng B, Sumkin JH, Zuley ML, Wang X, Klym AH, Gur D. Bilateral mammographic density asymmetry and breast cancer risk: a preliminary assessment. Eur J Radiol 2012;81:3222–8.
[27] Wang X, Lederman D, Tan J, Wang XH, Zheng B. Computerized prediction of risk for developing breast cancer based on bilateral mammographic breast tissue asymmetry. Med Eng Phys 2011;33:934–42.
[28] Wang X, Lederman D, Tan J, Wang XH, Zheng B. Computerized detection of breast tissue asymmetry depicted on bilateral mammograms: a preliminary study of breast risk stratification. Acad Radiol 2010;17:1234–41.
[29] Scutt D, Manning JT, Whitehouse GH, Leinster SJ, Massey CP. The relationship between breast asymmetry, breast size and the occurrence of breast cancer. Br J Radiol 1997;70:1017–21.
[30] Suri JS, Rangayyan RM. Recent advances in breast imaging, mammography, and computer-aided diagnosis of breast cancer, volume 155. SPIE press; 2006.
[31] Miller P, Astley SM. Detection of breast asymmetry using anatomical features. IS&T/SPIE's Symposium on Electronic Imaging: Science and Technology. International Society for Optics and Photonics; 1993. p. 433–42.
[32] Miller P, Astley S. Automated detection of breast asymmetry using anatomical features. State of the Art in Digital Mammographic Image Analysis, Series in Machine Perception and Artificial Intelligence, vol. 9. 1994. pp. 247–61.
[33] Ferrari RJ, Rangayyan RM, Desautels JEL, Borges RA, Frere AF. Automatic identification of the pectoral muscle in mammograms. IEEE Trans Med Imaging 2004;23:232–45.
[34] Torrents-Barrena J, Puig D, Melendez J, Valls A. Computer-aided diagnosis of breast cancer via gabor wavelet bank and binary-class svm in mammographic images. J Exp Theoret Artif Intell 2016;28:295–311.
[35] Evans KK, Haygood TM, Cooper J, Culpan A-M, Wolfe JM. A half-second glimpse often lets radiologists identify breast

cancer cases even when viewing the mammogram of the opposite breast. Proc Natl Acad Sci USA 2016;113:10292–7.
[36] Celaya-Padilla J, Martinez-Torteya A, Rodriguez-Rojas J, Galvan-Tejada J, Treviño V, Tamez-Peña J. Bilateral image subtraction and multivariate models for the automated triaging of screening mammograms. BioMed Res Int 2015;2015.
[37] Chan H-P, Wei D, Helvie MA, Sahiner B, Adler DD, Goodsitt MM, et al. Computer-aided classification of mammographic masses and normal tissue: linear discriminant analysis in texture feature space. Phys Med Biol 1995;40:857.
[38] Rosenfeld A. Multiresolution image processing and analysis, vol. 12. Springer Science & Business Media; 2013.
[39] Mattes D, Haynor DR, Vesselle H, Lewellyn TK, Eubank W. Nonrigid multimodality image registration. Medical Imaging 2001. International Society for Optics and Photonics; 2001. p. 1609–20.
[40] Rangayyan RM, Banik S, Desautels JEL. Computer-aided detection of architectural distortion in prior mammograms of interval cancer. J Dig Imaging 2010;23:611–31.
[41] Ibanez L, Schroeder W, Ng L, Cates J. The ITK software guide. Kitware; 2003.
[42] Ganesan K, Acharya UR, Chua KC, Min LC, Abraham KT. Pectoral muscle segmentation: a review. Comput Methods Programs Biomed 2013;110:48–57.
[43] Galván-Tejada CE, Zanella-Calzada LA, Galván-Tejada JI, Celaya-Padilla JM, Gamboa-Rosales H, Garza-Veloz I, et al. Multivariate feature selection of image descriptors data for breast cancer with computer-assisted diagnosis. Diagnostics 2017;7:9.
[44] Galván-Tejada CE, García-Vázquez JP, García-Ceja E, Carrasco-Jiménez JC, Brena RF. Evaluation of four classifiers as cost function for indoor location systems. Proc Comput Sci 2014;32:453–60.
[45] Heath M, Bowyer K, Kopans D, Moore R, Kegelmeyer P. The digital database for screening mammography. Proceedings of the 5th International Workshop on Digital Mammography; 2000. p. 212–8.
[46] López MAG, de Posada NG, Moura DC, Pollán RR, Valiente JMF, Ortega CS, et al. BCDR: a breast cancer digital repository. 15th International Conference on Experimental Mechanics; 2012.
[47] Beasley TM, Erickson S, Allison DB. Rank-based inverse normal transformations are increasingly used, but are they merited? Behav Genet 2009;39:580–95.
[48] Diez Y, Oliver A, Lladó Xavier, Freixenet J, Marti J, Vilanova JC, et al. Revisiting intensity-based image registration applied to mammography. IEEE Trans Inform Technol Biomed 2011;15:716–25.
[49] Martí R, Díez Y, Oliver A, Tortajada M, Zwiggelaar R, Lladó X. Detecting abnormal mammographic cases in temporal studies using image registration features. Breast Imaging. Springer; 2014. p. 612–9.
[50] Yin F, Giger ML, Doi K, Metz CE, Vyborny CJ, Schmidt RA. Computerized detection of masses in digital mammograms: analysis of bilateral subtraction images. Med Phys 1991;18:955–63.
[51] Rodriguez-Rojas J, Garza-Montemayor M, Trevino-Alvarado V, Tamez-Pena JG. Predictive features of breast cancer on Mexican screening mammography patients. SPIE Medical Imaging. International Society for Optics and Photonics; 2013. p. 867023–9.
[52] Tan M, Zheng B, Ramalingam P, Gur D. Prediction of near-term breast cancer risk based on bilateral mammographic feature asymmetry. Acad Radiol 2013;20:1542–50.

Please cite this article in press as: Celaya-Padilla JM, et al. Contralateral asymmetry for breast cancer detection: A CADx approach. Biocybern Biomed Eng (2017), https://doi.org/10.1016/j.bbe.2017.10.005